Water Air Soil Pollut (2021) 232: 99
https://doi.org/10.1007/s11270-021-05063-w

Oxalate Enhanced Organic Pollutant Removal with a UV/Fe^0 System: Performance, Mechanisms, and Role of Oxalate

Yuwei Pan · Zhuoyu Bu · Xiang Li · Jiangang Han

Received: 24 January 2021 / Accepted: 18 February 2021 / Published online: 26 February 2021

Abstract This study presented the efficient removal of tartrazine, a typical biorefractory dye, in a heterogeneous photochemical Fenton-like system adopting Fe^0 and oxalate (Ox) (UV/Fe^0/Ox). Only 47.4% tartrazine could be removed within 60 min with a UV/Fe^0 system. The addition of Ox could significantly enhance the removal of tartrazine to 72.4% within only 20 min with the UV/Fe^0/Ox system. The effects of various factors, such as the Fe^0 dose (0–0.8 g/L), Ox dose (0–2 mM), initial pH (2–6), and initial tartrazine concentration (2–30 mg/L), on the removal of tartrazine were examined. Scanning electron microscopy (SEM), Fourier transform infrared (FTIR) spectroscopy, and Mossbauer spectroscopy were conducted to explore the mechanism by which oxalate enhances the performance of the UV/Fe^0 system. Ox could inhibit the formation of iron (hydro)xides on the Fe^0 surface, thus guaranteeing the reactivity of Fe^0 during the reaction. Compared with Fe_2O_3, FeS, and Fe_3O_4, Fe^0 was a good heterogeneous iron catalyst for the photolysis of tartrazine with the Ox system. Compared with H_3PO_4, nitrilotriacetic acid, and ethylenediaminetetraacetic acid, Ox was also a good photolysis chelating agent. The UV/Fe^0/Ox system could also maintain fast tartrazine removal after five consecutive runs without the addition of Fe^0, indicating the good stability of Fe^0.

Keywords Tartrazine · Photochemical Fenton-like system · Fe^0 · Oxalate · Removal

Y. Pan (✉) · Z. Bu · J. Han
College of Biology and the Environment, Nanjing Forestry University, Nanjing 210037, China
e-mail: panyw@njfu.edu.cn

X. Li
School of Environment, Key Laboratory for Yellow River and Huai River Water Environment and Pollution Control, Ministry of Education, Henan Key Laboratory for Environmental Pollution Control, Henan Normal University, Xinxiang 453007, China

J. Han
Co-Innovation Center for the Sustainable Forestry in Southern China, Nanjing Forestry University, Nanjing 210037 Jiangsu, China

J. Han (✉)
National Positioning Observation Station of Hung-tse Lake Wetland Ecosystem in Jiangsu Province, Hongze, Huai'an 223100 Jiangsu, China
e-mail: hjg@njfu.edu.cn

1 Introduction

Currently, synthetic azo dye wastewater has attracted serious attention owing to its potential toxicity to the environment and humans (Chen et al. 2020; Pan et al. 2016). Among azo dyes, tartrazine is commonly used as a food coloring agent and is recalcitrant to biodegradation processes (Zhang et al. 2019a). Advanced oxidation processes (AOPs), which can generate powerful oxidative radicals, have generally been considered alternative methods for the treatment of nonbiodegradable and recalcitrant pollutants (Xu et al. 2020a; Li et al. 2019; Zhang et al. 2019b; Guo et al. 2020; Jiang et al. 2020;

Guo et al. 2021). Common oxidants that have been used include persulfate ($S_2O_8^{2-}$) (Li et al. 2018a; Li et al. 2020a), ozone (O_3) (Wang and Chen 2020), and hydrogen peroxide (H_2O_2) (Xu et al. 2020b).

Ox, as one of the dicarboxylic acids, is a common byproduct of most organic pollutants. The photolysis of an Fe-oxalate (Fe-Ox) complex has attracted much attention for effectively degrading different recalcitrant and nonbiodegradable pollutants via Eqs. (1–6) (Huang et al. 2017). The use of heterogeneous iron catalysts are advantageous compared with homogeneous iron salts because of the low production of ferric ions and the recycling of solids (Huang et al. 2017). Many heterogeneous iron catalysts have been adopted for the photolysis of ferric-oxalate complexes, such as maghemite (γ-Fe_2O_3) (Dai et al. 2018), goethite (α-FeOOH) (Lan et al. 2010), magnetite (Fe_3O_4) (Huang et al. 2017), and hematite (α-Fe_2O_3) (Lan et al. 2016). Currently, a large number of studies have focused on wastewater treatment by zero-valent iron (Fe^0) because Fe^0 is abundant, inexpensive, and environmentally friendly (Li et al. 2018b; Pan et al. 2020a). Our previous studies reported that Ox could enhance the activation of O_2 in the Fe^0/O_2 system, thus improving H_2O_2 production (Pan et al. 2020b); additionally, ethylenediaminetetraacetic acid and nitrilotriacetic acid could modify the surface characteristics of Fe^0 in the absence of UV (Pan et al. 2020b; Pan et al. 2019). Therefore, the photolysis of Ox catalyzed by Fe^0 might exhibit good performance for pollutant removal.

$$Fe^{III}(C_2O_4)n^{3-2n} + hv \rightarrow Fe^{II} + (n-1)C_2O_4^{2-} + C_2O_4 \quad (1)$$

$$C_2O_4^- + O_2 \rightarrow 2CO_2 + O_2 \quad (2)$$

$$O_2 \leftrightarrow HO_2 (pH-dependent) \quad (3)$$

$$O_2^-/HO_2 + H^+ \rightarrow H_2O_2 + O_2 \quad (4)$$

$$O_2^-/HO_2 + H^+ + Fe^{2+} \rightarrow H_2O_2 + O_2 + Fe^{3+} = \pi r^2 \quad (5)$$

$$Fe^{II}[(C_2O_4)n]^{3-2n} + H_2O_2 \rightarrow Fe^{III}[(C_2O_4)n]^{3-2n} + OH + OH^- \quad (6)$$

A heterogeneous photochemical Fe^0/Ox system (UV/Fe^0/Ox) system was investigated in the present study for tartrazine removal. The objectives of the present study are listed as follows: (1) investigate the efficiency of tartrazine removal with the UV/Fe^0/Ox system; (2) explore the affecting factors, such as the Fe^0 dose, Ox dose, initial pH, and initial tartrazine concentration on tartrazine removal; (3) investigate the mechanism on tartrazine removal in the UV/Fe^0/Ox system; (4) investigate the effect of Ox on the modification of the Fe^0 surface; (5) clarify the effect of the H_2O_2 addition on removing tartrazine with the UV/Fe^0/Ox system; (6) explore the performance of various chelating agents and catalysts for tartrazine removal; and (7) investigate the recycling of Fe^0 for tartrazine removal.

2 Materials and Methods

2.1 Chemicals

Oxalate, $FeSO_4$, $Fe_2(SO_4)_3$, H_2O_2 (30%), catalase (CAT), superoxide dismutase (SOD), methanol (HPLC-grade), and phenanthroline were purchased from Aladdin (China). Tartrazine was purchased from Meryer Chemical Technology Co., Ltd. Fe^0, Fe3O4, FeS, and Fe_2O_3 were purchased from Shanghai Jinshan Co.

2.2 Tartrazine Removal Experiments

Experiments were performed in 500 mL of working solution, containing Fe^0 (0–0.8 g/L), Ox (0–2 mM), and tartrazine (2–30 mg/L) and stirred by a mechanical stirrer. The experiment was initiated by placing a preheated UV lamp (GPH150T5L/5 W/254 nm from Kadind) sealed in a glass sleeve into the working solution.

2.3 Analytical Methods

Concentrations of tartrazine were detected by a UV-visible spectrophotometer (Shanghai Mapada Company, P1) at 428 nm. The H_2O_2 concentration was detected by the potassium titanium oxalate method at 400 nm. The concentration of total Fe was detected by inductively coupled plasma optical emission spectrometry (Agilent 720ES, USA). Ox was measured by an ion chromatograph (ICS-900, Thermo Fisher Scientific). A morphological analysis of Fe^0 species was obtained by SEM (Hitachi 4700 microscope) with a combined EDX

analyzer (EDX). FTIR spectroscopy was conducted by an FTIR-840OS Shimadzu spectrophotometer (Japan) from 500 to 4000/cm. Mossbauer spectroscopy of Fe^0 was analyzed using the MossWin 4.0 program.

Pollutant removal (η/%) was calculated according to Eq. (7), the removal rate pollutant (k) was fitted by the pseudo-first-order rate equation (Eq. (8)).

$$\eta = \frac{C_0 - C_t}{0} x100\% \quad (7)$$

$$\ln C_t / C_0 = -kt \quad (8)$$

where k is the degradation rate and C_0 (mg/L) and C_t (mg/L) are the concentrations of the pollutant at time 0 and at the reaction time (t), respectively.

To demonstrate the role of oxalate, the value of f was calculated via Eq. (9).

$$f = k_1 / k_2 \quad (9)$$

where k_1 and k_2 are the pseudo-first-order constants for removing pollutants in the UV/Fe^0/Ox and UV/Fe^0 systems, respectively.

3 Results and Discussion

3.1 Tartrazine Removal with the Different Systems

Tartrazine removal, Ox removal, Fe-ion generation, and H_2O_2 production were compared with the different systems. As shown in Fig. 1a, 27.1% of tartrazine could be removed within 60 min by only Fe^0, which, due to reactive oxygen species, could be generated via the activation of O_2 by Fe^0 (Pan et al. 2020b). The addition of Ox could enhance the activation of O_2, thus increasing H_2O_2 production, while Ox could also compete with tartrazine for $^{\bullet}OH$ (Pan et al. 2020b). Thus, compared with the Fe^0 system, the tartrazine removal increased only slightly in the Fe^0/Ox system (28.6%). Under UV irradiation alone, 32.6% of tartrazine could be removed within 60 min, indicating that the direct photolysis of tartrazine occurred, whereas 47.4% of tartrazine could be removed within 60 min when UV was combined with Fe^0, which might be because the H_2O_2 generated by the activation of O_2 could be catalyzed under UV irradiation. Thus, formic acid (HOCOH) could be generated by reacting with O_2 to form H_2O_2 during the photolysis of Ox (Jiang et al. 2017). Furthermore, H_2O_2 could be converted in $^{\bullet}OH$ for removing pollutants under UV irradiation. However, only 27.1% of tartrazine could be removed within 60 min in the UV/Ox system, which might be because of the competition between tartrazine and Ox for $^{\bullet}OH$. Additionally, 72.4% of tartrazine could be removed within only 20 min in the UV/Fe^0/Ox system owing to the reactions outlined in Eqs. (1–6), while tartrazine could not be further removed after 20 min which might because the tartrazine degradation intermediates generated during the reaction competing with the $^{\bullet}OH$ radical. Moreover, as shown in Fig. 1b, the value of k (10^3) for removing tartrazine with the UV/Fe^0/Ox system (59.5 min^{-1}) was much higher than with the Fe^0/Ox (3.5 min^{-1}), Fe^0 (6.9 min^{-1}), UV (5.9 min^{-1}), UV/Fe^0 (10.9 min^{-1}), and UV/Ox (6.7 min^{-1}) systems. Moreover, the Ox removal with the UV/Fe^0/Ox system was also much faster than with the Fe^0/Ox and UV/Ox systems.

The total concentration of Fe ions generated with the different systems was also detected. As depicted in Fig. 1d, the total concentrations of Fe ions generated with the UV/Fe^0/Ox system (10.4 mg/L) were also much higher than those with the Fe (5.3 mg/L), Fe^0/Ox (6.4 mg/L), and UV/Fe^0 (5.9 mg/L) systems. The generated Fe ions could induce the photolysis reaction Eqs. (1–6), thus increasing H_2O_2 production. As shown in Fig. 1e, H_2O_2 production with the UV/Fe^0/Ox system (22.8 μM) was also much higher than that with the Fe^0 (0.43 μM), Fe^0/Ox (7.7 μM), and UV/Fe^0 (0.54 μM) systems. The presence of more H_2O_2 with UV/Fe^0/Ox could induce more $^{\bullet}OH$ generation for pollutant removal.

3.2 Effect of Various Affecting Factors

3.2.1 Ox Concentration

Ox could react with Fe^{III} and Fe^{II} to form Fe-Ox complexes, thus inducing Eqs. (1–6), while Ox could also compete with tartrazine for $^{\bullet}OH$. Thus, the effect of the Ox concentration (0–2 mM) on the removal of tartrazine was determined. As shown in Fig. 2a, the tartrazine removal increased with an increasing Ox concentration. The tartrazine removal within 60 min increased from 47.4 to 87.2%, while the Ox dose increased from 0 to 1 mM and then decreased to 85.5% at a 2-mM Ox dose. As depicted in Fig. 2b, the value of k (10^3) also increased from 10.9 to 82.2 min^{-1}, while the Ox concentration increased from 0 to 1 mM and then decreased to

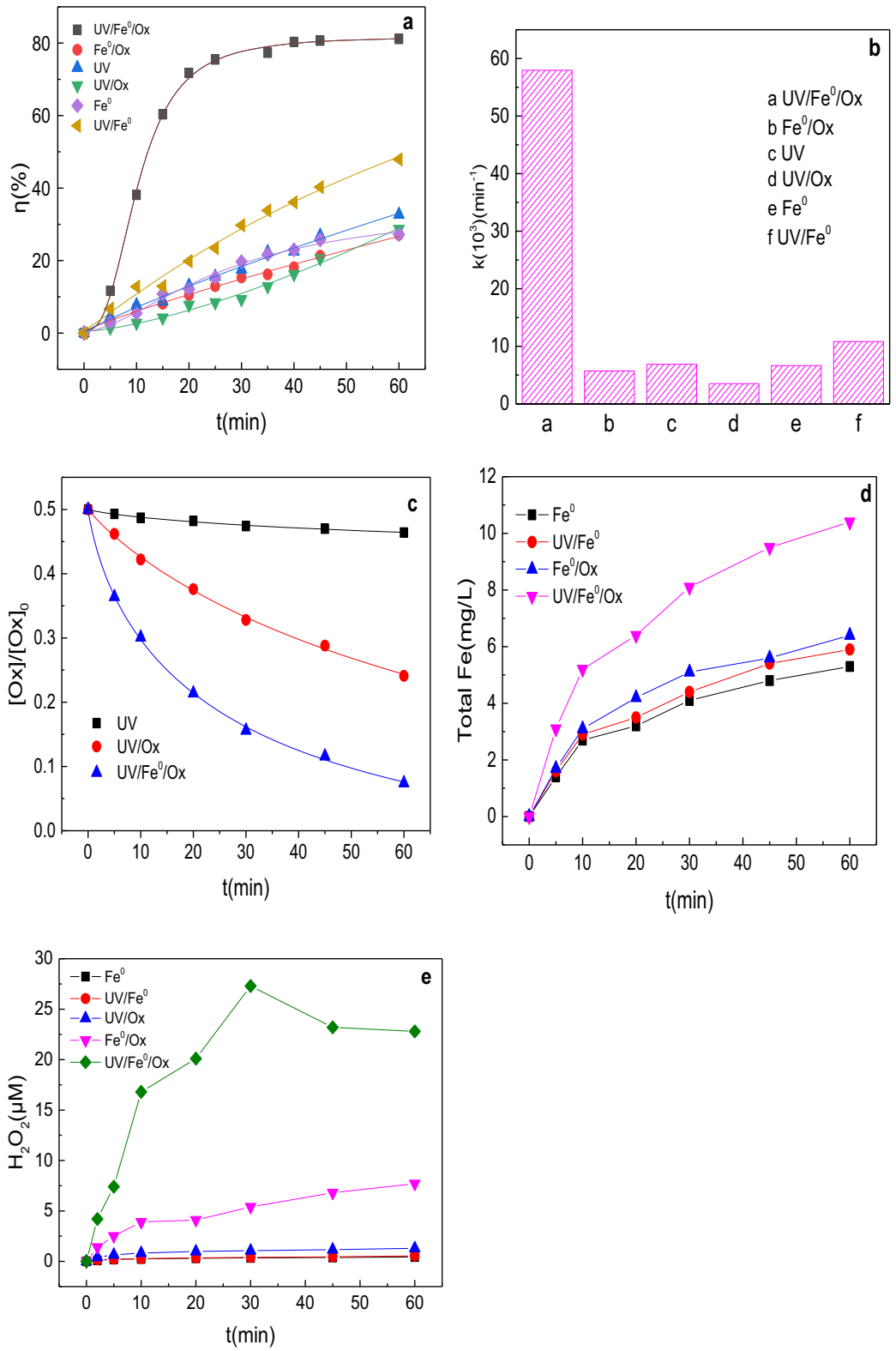

Fig. 1 (**a**) Removal of tartrazine, (**b**) removal of Ox, (**c**) value of k (10^3), (**d**) generation of total Fe, and (**e**) H_2O_2 generation with the different systems. Reaction conditions: [Fe^0] 0.2 g L^{-1}, [Ox] 0.5 mM, pH 4, and [tartrazine] 20 mg L^{-1}

78.4 min^{-1} at a 2-mM Ox dose. Therefore, the optimal Ox dose was 1 mM.

3.2.2 Initial pH

The initial pH could not only affect the Fe^0 corrosion rate but also affect the species of the Fe-Ox complex. Fe^{II} and $[Fe^{II}(C_2O_4)_2]^{2-}$ were regarded as Fe^{II}-Ox complexes at pH < 3 and pH ≥ 3, respectively. $Fe^{III}(C_2O_4)_2]^+$, $[Fe^{III}(C_2O_4)_2]^-$, $[Fe^{III}(C_2O_4)_3]^{2-}$, and $Fe(OH)_3$ were regarded as Fe^{III}-Ox complexes at pH < 2, pH 2–6, and pH > 6, respectively (Zhou et al. 2014). Figure 2c and d present the tartrazine removal at different initial pH values from 2 to 6, and the best performance was achieved at the initial pH of 3–4, which was due to $[Fe^{III}(C_2O_4)_2]^-$ and $[Fe^{III}(C_2O_4)_3]^{2-}$ being the dominant Fe^{III}-Ox complexes that contained high photoactivity at pH 3–4. The value of k at pH 2 was lower than that at pH 3 because the reaction between Fe^{II}(pH 2) and H_2O_2 was much lower than the reaction between $[Fe^{II}(C_2O_4)_2]^{2-}$ (pH ≥ 3) and H_2O_2 (Zhou et al. 2014).

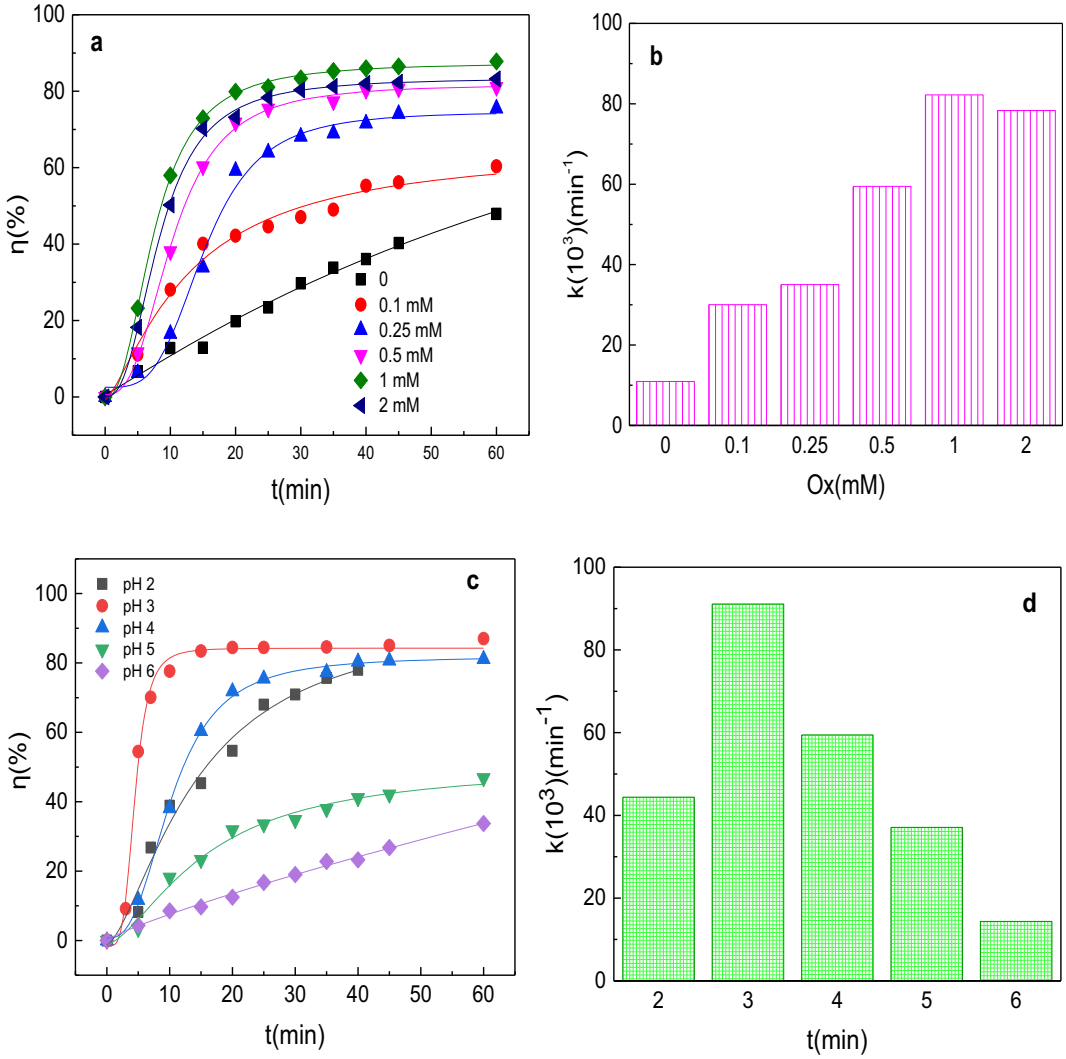

Fig. 2 **a** Removal of tartrazine at different Ox concentrations. **b** Value of k (10^3) at different Ox concentrations. **c** Removal of tartrazine at different initial pH values. **d** Value of k (10^3) at different initial pH values. **e** Removal of tartrazine at different Fe^0 doses. **f** Value of k (10^3) at different Fe^0 doses. **g** Removal of tartrazine at different tartrazine concentrations. **h** Value of k (10^3) at different tartrazine concentrations. Reaction conditions: [Fe^0] 0.2 g L^{-1}, [Ox] 0.5 mM, pH 4, and [tartrazine] 20 mg L^{-1}

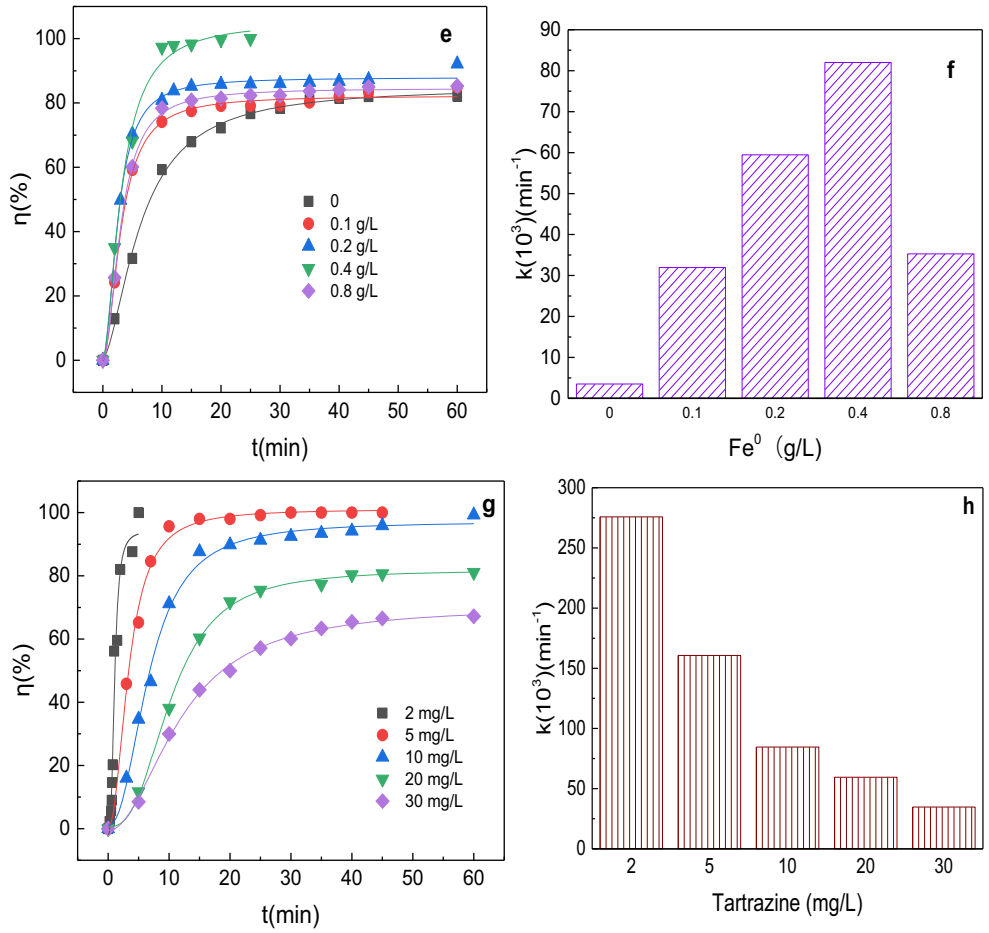

Fig. 2 (continued)

3.2.3 Fe^0 Dose

The Fe^0 dose affected the soluble iron concentration, thus influencing the Fe-Ox complex concentration. Figure 2e and f depict the tartrazine removal and value of *k* at different Fe^0 doses (0–0.8 g/L). The tartrazine removal and the value of *k* that increased with the Fe^0 dose were enhanced because more Fe-Ox complexes could catalyze H_2O_2 faster. An excessive Fe^{2+} concentration would also inhibit $^{\bullet}OH$, thus decreasing the removal of tartrazine (Pan et al. 2016). Therefore, the optimal Fe^0 dose was 0.4 g/L.

3.2.4 Initial Tartrazine Concentration

Tartrazine concentrations were different in various dye wastewaters; thus, the effect of the initial tartrazine concentration (varying from 2 to 30 mg/L) on the removal of tartrazine was investigated. As depicted in Fig. 2g and h, the tartrazine removal and value of *k* increased while the initial tartrazine concentration decreased. When the initial tartrazine concentration was 2 mg/L, the removal could reach 100% within only 2 min. A total of 67.2% tartrazine could still be removed within 60 min when the initial tartrazine concentration was 30 mg/L.

3.3 Mechanism Discussion

3.3.1 Reactive Oxygen Species

To determine the main radicals for the removal of tartrazine in the UV/Fe^0/Ox system, superoxide dismutase (SOD), catalase (CAT), and methanol (MA) were selected for quenching $O_2^{\bullet-}$, H_2O_2, and $^{\bullet}OH$, respectively (Song et al. 2019). As depicted in Fig. 3a and b, when SOD, CAT, and MA were added, the tartrazine removal decreased from 81.1 to 77.6,

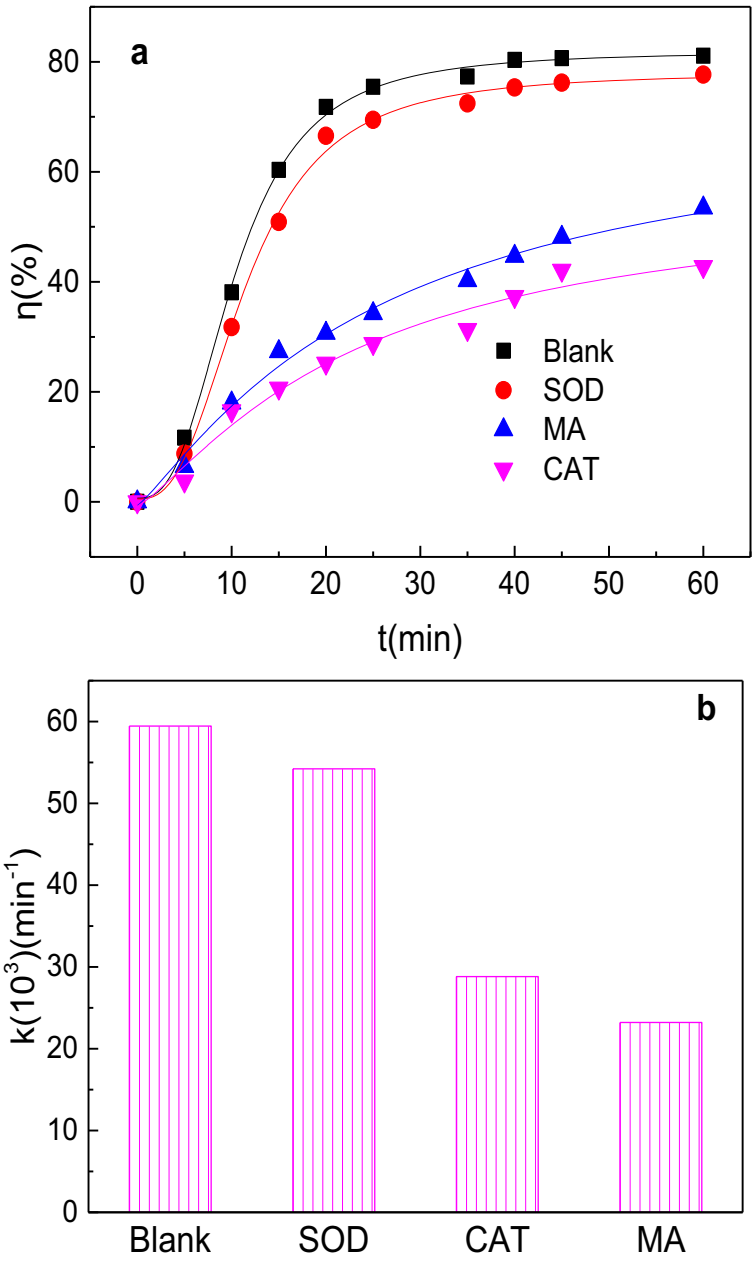

Fig. 3 **a** Tartrazine removal with different scavengers in the UV/Fe^0/Ox system. **b** Value of *k* for tartrazine removal with different scavengers in the UV/Fe^0/Ox system. Reaction conditions: [Fe^0] 0.2 g L^{-1}, [Ox] 0.5 mM, pH 4, and [tartrazine] 20 mg L^{-1}; MA 2 M, SOD of 3000 U L^{-1}, and CAT of 200,000 units L^{-1}

53.4, and 42.8% with the corresponding values of *k* (10^3) decreasing from 59.5 to 54.2, 28.8 and 23.2 min^{-1}. The order of scavengers in suppressing tartrazine removal was MA> CAT >SOD. The inhibitory efficiency (λ) values of the three scavengers were calculated via Eq. (10), and these values were 8.9, 51.6, and 61.1% for SOD, CAT, and MA, respectively. These results demonstrated that $^{\bullet}OH$ was the major radical for the removal of tartrazine, H_2O_2 was the major intermediate for $^{\bullet}OH$ generation, and $O_2^{\bullet-}$ played a minor role in the removal of tartrazine.

$$\lambda = \left(\left(k - k_q\right)/k\right) * 100\% \quad (10)$$

where *k* and k_q refer to the values of *k* in the absence and presence of the quenching agents.

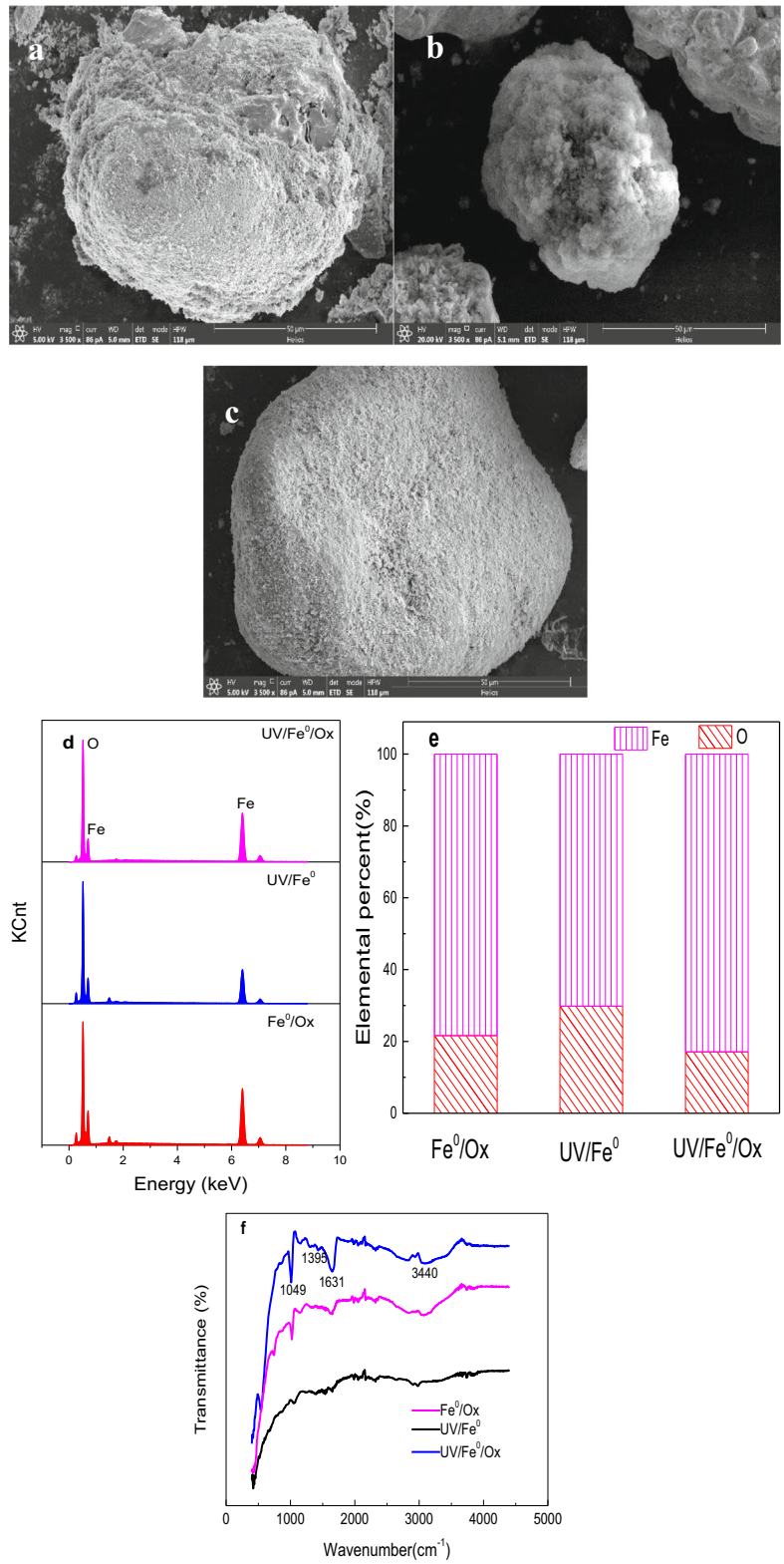

Fig. 4 SEM spectra of Fe^0 after 60 min of reacting with the (**a**) Fe^0/Ox, (**b**) UV/Fe^0, and (**c**) UV/Fe^0/Ox systems; (**d**) EDX pattern, (**e**) elemental percentages, and (**f**) FTIR pattern of Fe^0 after 60 min with the different systems. Reaction conditions: [Fe^0] 0.2 g L^{-1}, [Ox] 0.5 mM, pH 4, and [tartrazine] 20 mg L^{-1}

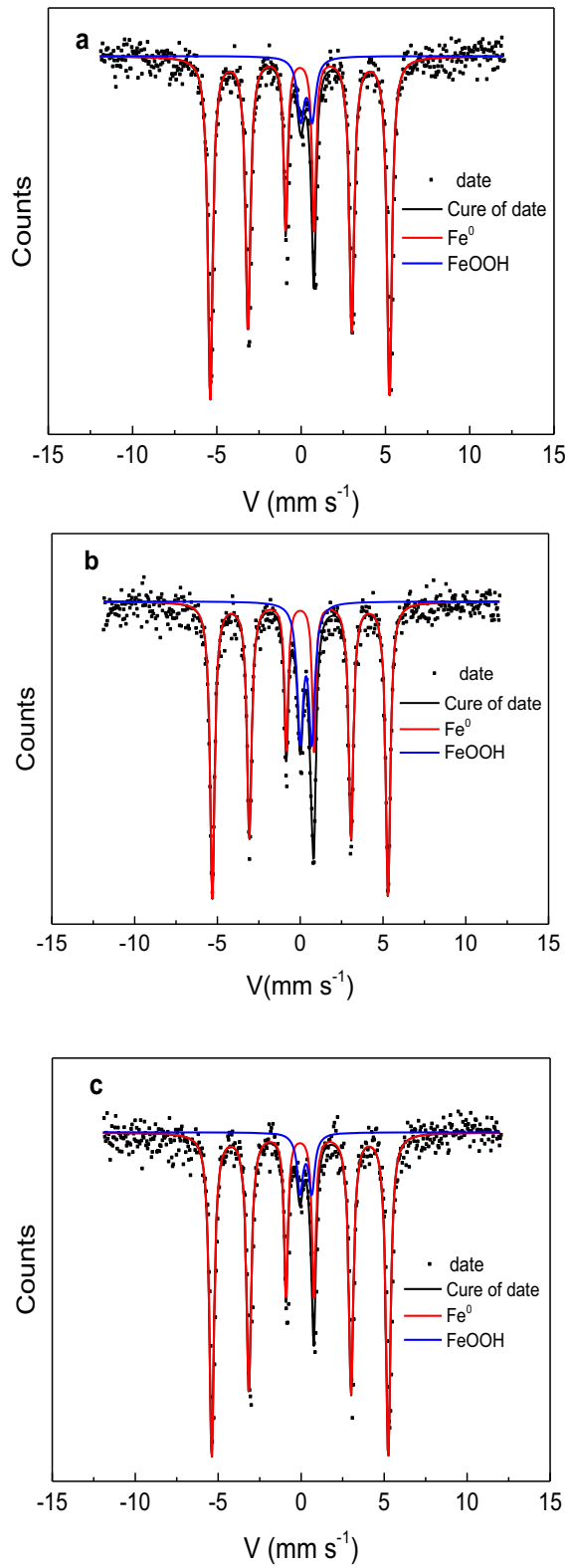

Fig. 5 Mossbauer spectra of Fe^0 after 60 min with the (**a**) Fe^0/Ox, (**b**) UV/Fe^0, and (**c**) UV/Fe^0/Ox systems. Reaction conditions: [Fe^0] 0.2 g L^{-1}, [Ox] 0.5 mM, pH 4, and [tartrazine] 20 mg L^{-1}

3.3.2 SEM-EDX and FTIR

The SEM images of Fe^0 after 60 min of reaction with the Fe^0/Ox, UV/Fe^0, and UV/Fe^0/Ox systems are presented in Fig. 4a–c. As shown in Fig. 4b, the surface of Fe^0 was much coarser with the UV/Fe^0 system than with the Fe^0/Ox system (Fig. 4a) and UV/Fe^0/Ox system (Fig. 4c). Fe-oxide corrosion products could cover the Fe^0 surface during the reaction, thus inhibiting the Fe^0 corrosion rate. However, the formation of Fe^0-Ox complexes could inhibit the covering of the Fe^0 surface by Fe oxides, thus guaranteeing the reactivity of Fe^0. Moreover, as shown in Fig. 4d and e, the O content of the reacted Fe^0 with the UV/Fe^0 system (29.8%) was larger than that in the Fe^0/Ox (17.1%) and UV/Fe^0/Ox (21.6%) systems. These results demonstrated that more corrosion products covered the Fe^0 surface with the UV/Fe^0 system, which would inhibit the Fe^0 corrosion rate.

The FTIR spectra of Fe^0 after 60 min of reaction with the Fe^0/Ox, UV/Fe^0, and UV/Fe^0/Ox systems were also detected (Fig. 4f). The obtained signals recorded at 1049, 1395, 1631, and 3440 cm^{-1} corresponded to C-O, -COO-, C=O, and O-H, respectively (Chong et al. 2016., Guan et al. 2015; Repo et al. 2013; Bennet et al. 2016). The high intensity of these oxygen-containing groups when reacting with the UV/Fe^0/Ox system demonstrated the formation of the Fe-Ox complex on the Fe^0 surface.

3.3.3 Mossbauer Spectra Analysis

Mossbauer spectroscopy was conducted as a quantitative method to inspect the Fe species deposited on the reacted Fe^0 with different systems. As depicted in Fig. 5, there were two distinguishable compositions within the structure: a prevailing sextet line referenced to Fe^0 and a doublet line referenced to FeOOH (Li et al. 2020b). Additionally, FeOOH might be formed according to Eq. (11). The percentages of FeOOH were 9.3, 20.9, and 10.2% with the Fe^0/Ox, UV/Fe^0, and UV/Fe^0/Ox systems, respectively. Thus, more corrosion products

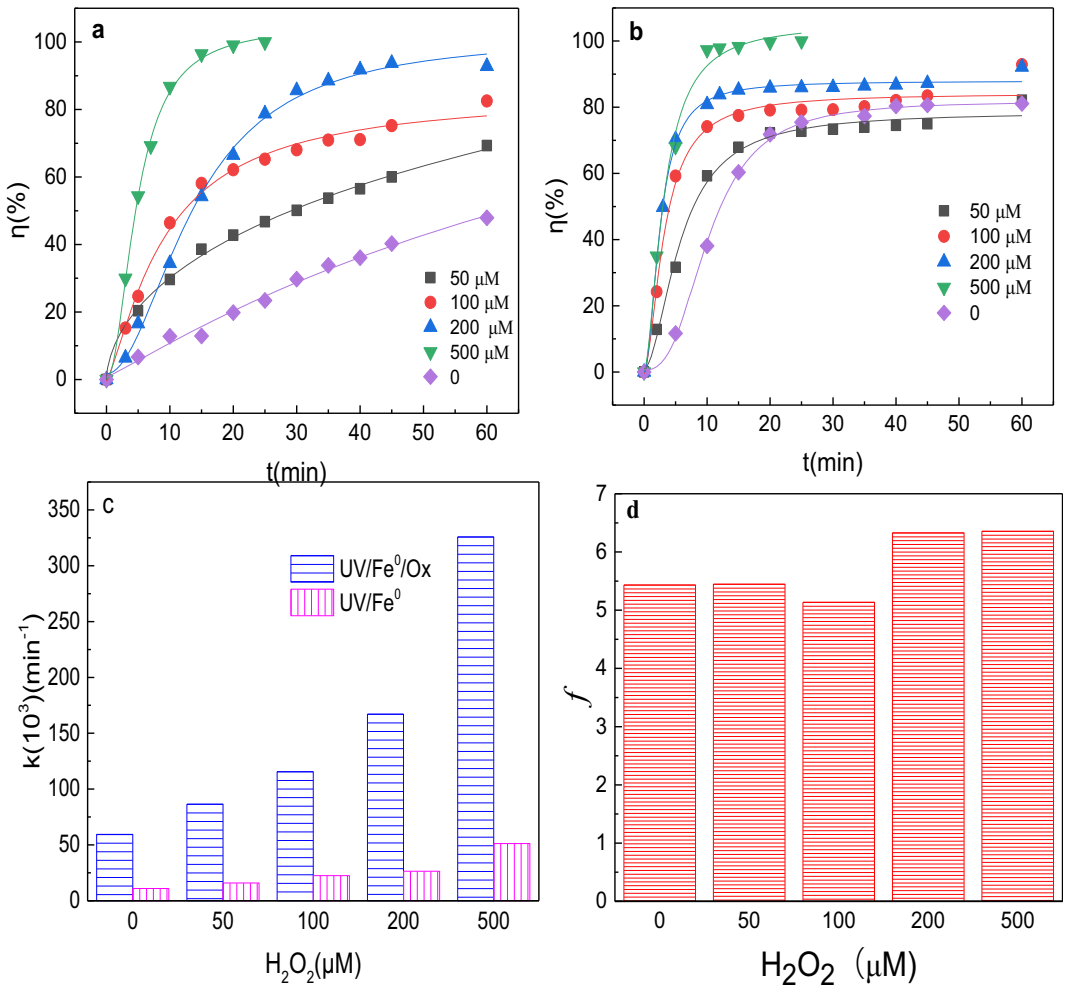

Fig. 6 **a** Tartrazine removal with the UV/Fe^0/Ox system and a H_2O_2 addition. **b** Value of *k* for tartrazine removal with the UV/Fe^0/Ox system and a H_2O_2 addition. **c** Tartrazine removal with the UV/Fe^0 system and a H_2O_2 addition. **d** Value of *k* for tartrazine removal with the UV/Fe^0 system and a H_2O_2 addition

covering the reacted Fe^0 with the UV/Fe^0 system might inhibit the reactivity of Fe^0, and these results were consistent with the SEM results.

$$2Fe^{2+} + 1/2\ O_2 + 3\ H_2O \rightarrow 2\ FeOOH + 4\ H^+ \quad (11)$$

3.4 Effect of a H_2O_2 Addition

H_2O_2 was the major intermediate for $^{\bullet}OH$ generation; thus, we investigated the effect of a H_2O_2 addition on the removal of tartrazine with both the UV/Fe^0 and UV/Fe^0/Ox systems. As depicted in Fig. 6a and b, the H_2O_2 addition could significantly enhance the tartrazine removal with both systems; this result was due to the additional H_2O_2 improving the generation of $^{\bullet}OH$. Fig. 6c presents the value of *k* with different H_2O_2 additions to both systems. When the H_2O_2 addition increased from 0 to 50, 100, 200, and 500 μM, the values of *k* (10^3) increased from 10.9 to 15.9, 22.5, 26.4, and 51.3min^{-1} with the UV/Fe^0 system and from 59.5 to 86.5, 115.6, 167.2, and 325.9 min^{-1} with the UV/Fe^0/Ox system, respectively. Compared with the UV/Fe^0 system, the value of *k* could be significantly enhanced with the UV/Fe^0/Ox system, and the value of *f* could remain at approximately 5.1–6.4 at any H_2O_2 dose (Fig. 6d). These results might be because the reaction rate between $[Fe^{II}(C_2O_4)_2]^{2-}$ and H_2O_2 proceeded at a rate 3–4 orders of magnitude faster than that between Fe^{II}

and H_2O_2. Therefore, the H_2O_2 addition could significantly enhance the removal of tartrazine with the UV/Fe^0/Ox system.

3.5 Comparing Various Catalysts and Chelating Agents

The performance of various catalysts adopted in the photolysis of ferric-oxalate complexes was compared. As shown in Fig. 7a, the tartrazine removal within 60 min was 35.9, 67.5, 69.4, 70.7, 81.1, and 86.4% with the UV/Fe_2O_3/Ox, UV/FeS/Ox, UV/Fe_3O_4/Ox, UV/Fe^{III}/Ox, UV/Fe^0/Ox, and UV/Fe^{II}/Ox systems, respectively. The increase in the value of k (10^3) on the tartrazine removal increased in the following order: Fe_2O_3 (10.7 min^{-1}) < FeS (26.3 min^{-1}) < Fe_3O_4 (42.4 min^{-1}) < Fe^{III} (47.3 min^{-1}) < Fe^0 (59.5 min^{-1}) < Fe^{II} (77.1 min^{-1}) (Fig. 7b). Compared with other heterogeneous iron catalysts, Fe^0 could have a higher tartrazine removal and faster tartrazine removal rate. Compared with heterogeneous iron catalysts, Fe^0 obtained a similar tartrazine removal efficiency and tartrazine removal rate. Therefore, Fe^0 was a good heterogeneous iron catalyst for the photolysis of pollutants with the Ox system.

To clarify the photolysis performance of various chelating agents, the tartrazine removal with different UV/Fe^0/chelating agents was compared. As depicted in Fig. 7c, the tartrazine removal within 60 min was 19.3, 58.7, 78.4, and 81.1% with the UV/Fe^0/H_3PO_4, UV/Fe^0/EDTA, UV/Fe^0/NTA, and UV/Fe^0/Ox

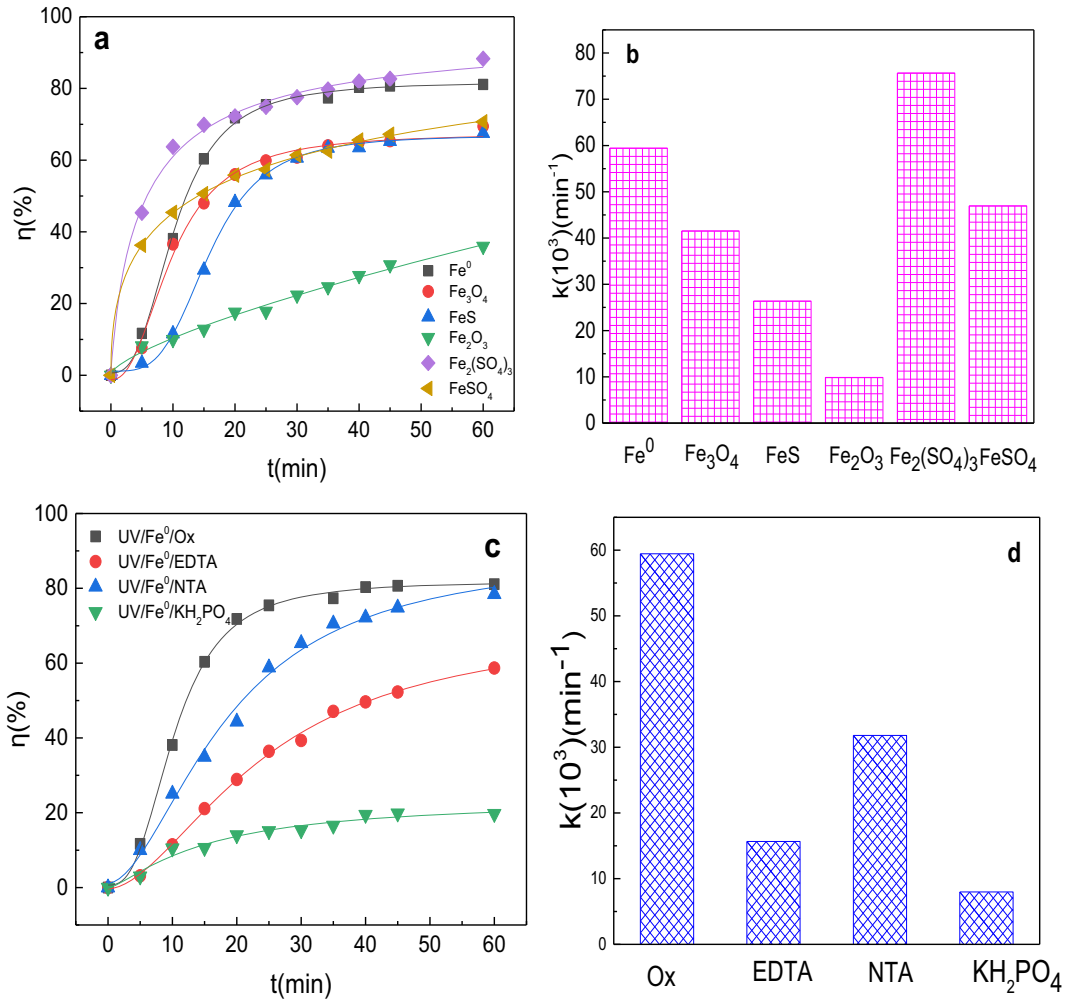

Fig. 7 **a** Tartrazine removal with different Fe source systems. **b** Value of k for tartrazine removal with different Fe source systems. **c** Tartrazine removal with different chelating agent systems. **d** Value of k for tartrazine removal with different chelating agent systems. Reaction conditions: [catalysts] 0.2 g L^{-1}, [chelating agent] 0.5 mM, pH 4, and [tartrazine] 20 mg L^{-1}

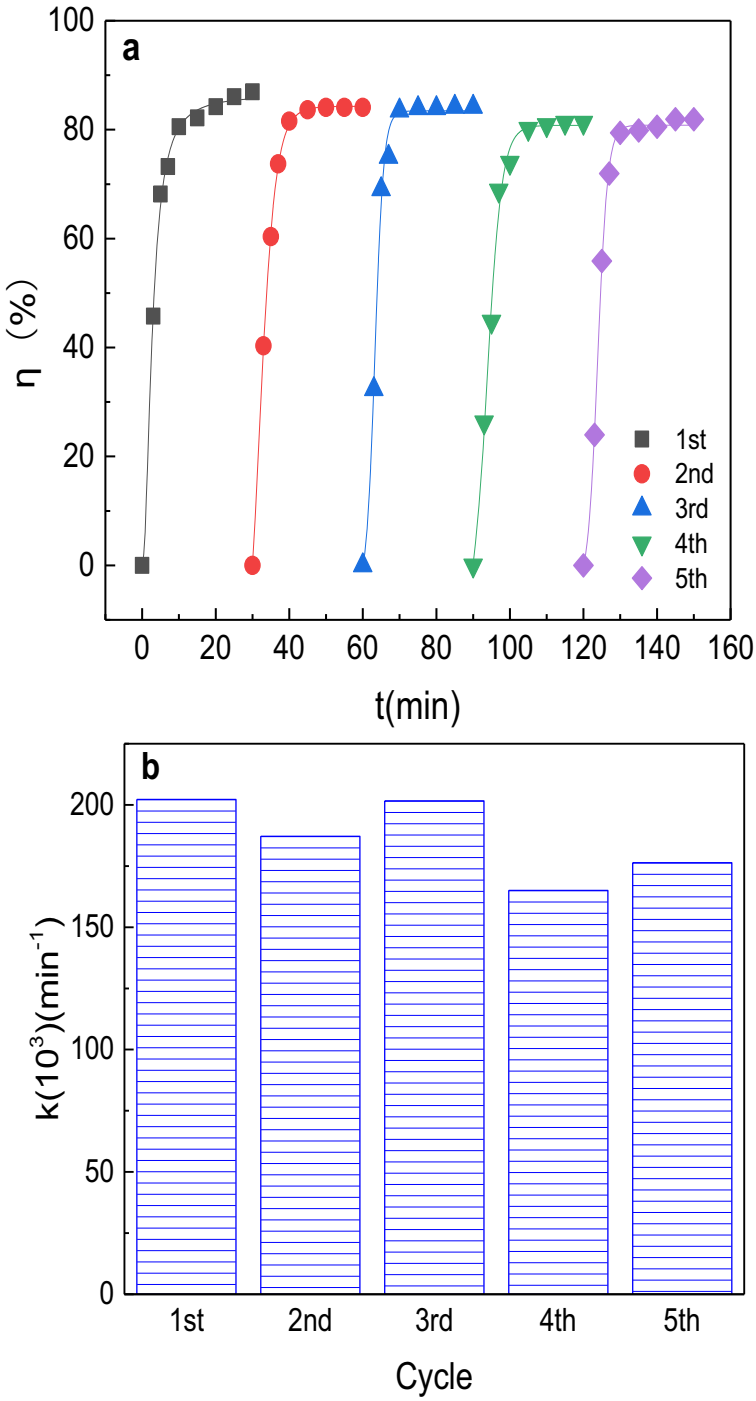

Fig. 8 Repeated runs with the UV/pre-Fe^0/Ox system: (**a**) tartrazine removal and (**b**) *k* values. Reaction conditions: [Fe^0] 0.2 g L^{-1}, [Ox] 0.5 mM, pH 4, and [tartrazine] 10 mg L^{-1}

systems, respectively. The increase in the value of *k* (10^3) on the tartrazine removal increased in the following order: H_3PO_4 < EDTA < NTA < Ox (59.5 min^{-1}) (Fig. 7d). Thus, Ox was a good photolysis chelating agent.

3.6 Reusability of Fe^0

Fe^0 could be a good heterogeneous iron catalyst for the photolysis of tartrazine with the Ox system; thus, it is critical to examine the recyclability of the catalyst for

long-term use. To assess the reusability of Fe^0 in the UV/Fe^0/Ox system, five consecutive experiments of tartrazine removal were conducted under the same reaction conditions. As presented in Fig. 8a, after five consecutive experiments, the tartrazine removal within 30 min was 86.9, 84.1, 84.2, 81.3, and 81.9%, respectively. The values of k (10^3) were 202.6, 187.2, 201.7, 165.2, and 176.4 min^{-1} in the 1st, 2nd, 3rd, 4th, and 5th runs, respectively (Fig. 8b). These results demonstrated that Fe^0 showed good stability for long-term operation.

4 Conclusion

In this study, Ox was adopted to enhance a UV/Fe^0 system for the removal of tartrazine. Only 47.4% of tartrazine could be removed within 60 min with the UV/Fe^0 system, while 72.4% of tartrazine could be removed within only 20 min with the UV/Fe^0/Ox system. The effects of various factors, such as the Fe^0 dose (0–0.8 g/L), Ox dose (0–2 mM), initial pH (2–6), and initial tartrazine concentration (2–30 mg/L), on the tartrazine removal were examined. The optimal Fe^0 dose, Ox dose, and initial pH were 0.4 g/L, 1 mM, and pH 3, respectively. Quenching experiments demonstrated that $^{\bullet}OH$ was the major radical for the removal of tartrazine, H_2O_2 was the major intermediate for $^{\bullet}OH$ generation, and $O_2^{\bullet-}$ played a minor role in tartrazine removal. SEM-EDX, FTIR, and Mossbauer spectroscopy were conducted to explore the mechanism by which oxalate enhanced the performance of the UV/Fe^0 system. Ox could inhibit the formation of iron (hydro)xides on the Fe^0 surface, thus guaranteeing the reactivity of Fe^0 during the reaction. Compared with Fe_2O_3, FeS, and Fe_3O_4, Fe^0 was a good heterogeneous iron catalyst for the photolysis of pollutants with the Ox system. Compared with H_3PO_4, nitrilotriacetic acid, and ethylenediaminetetraacetic acid, Ox was also a good photolysis chelating agent. Finally, Fe^0 showed good stability for long-term operation with the UV/Fe^0/Ox system.

Author's Contribution Yuwei Pan: Conceptualization, methodology, formal analysis, investigation, data curation, writing original draft, and writing review and editing. Zhuoyu Bu: investigation and resources. Xiang Li: investigation and resources. Jiangang Han: supervision, funding acquisition, and resources.

Funding This study was financially supported by the National Key Research and Development Project (2017YFC0505803) and the National Natural Science Foundation of China (No. 41977354). This study was also financially supported by the Priority Academic Program Development of Jiangsu Higher Education Institutions (PAPD).

Data Availability Not applicable.

Declarations

Ethics Approval and Consent to Participate Not applicable.

Consent for Publication Not applicable.

Competing Interests The authors declare no competing interests.

References

Bennet, J., Tholkappiyan, R., Vishista, K., Jaya, N. V., & Hamed, F. (2016). Attestation in self-propagating combustion approach of spinel AFe_2O_4 (A = Co, Mg and Mn) complexes bearing mixed oxidation states: Magnetostructural properties. *Applied Surface Science, 383*, 113–125.

Chen, R. P., Cai, J. L., Li, Q., Wei, X. Y., Min, H. H., & Yong, Q. (2020). Coadsorption behaviors and mechanisms of Pb(ii) and methylene blue onto a biodegradable multi-functional adsorbent with temperature-tunable selectivity. *RSC Advances, 10*, 35636–35645.

Chong, S., Zhang, G., Tian, H., & Zhao, H. (2016). Rapid degradation of dyes in water by magnetic Fe(0)/Fe_3O_4/graphene composites. *Journal of Environmental Sciences, 44*, 148–157.

Dai, H. W., Xu, S. Y., Chen, J. X., Miao, X. Z., & Zhu, J. X. (2018). Oxalate enhanced degradation of Orange II in heterogeneous UV-Fenton system catalyzed by Fe_3O_4 @γ-Fe_2O_3 composite. *Chemosphere, 199*, 147–153.

Guan, X., Jiang, X., Qiao, J., & Zhou, G. (2015). Decomplexation and subsequent reductive removal of EDTA-chelated CuII by zero-valent iron coupled with a weak magnetic field: Performances and mechanisms. *Journal of Hazardous Materials, 300*, 688–694.

Guo, H., Li, Z., Zhang, Y., Jiang, N., Wang, H. J., & Li, J. (2020). Degradation of chloramphenicol by pulsed discharge plasma with heterogeneous Fenton process using Fe_3O_4 nanocomposites. *Separation and Purification Technology, 253*, 117540.

Guo, H., Li, Z., Lin, S. Y., Li, D. S., Jiang, N., Wang, H. J., Han, J. G., & Li, J. (2021). Multi-catalysis induced by pulsed discharge plasma coupled with graphene-Fe_3O_4 nanocomposites for efficient removal of ofloxacin in water: Mechanism, degradation pathway and potential toxicity. *Chemosphere, 265*, 129089.

Huang, M., Zhou, T., Wu, X., & Mao, J. (2017). Distinguishing homogeneous-heterogeneous degradation of norfloxacin in a photochemical Fenton-like system (Fe_3O_4/UV/oxalate) and

the interfacial reaction mechanism. *Water Research, 119*, 47–56.

Jiang, B., Xin, S., He, H., Liu, X., Gao, L., Tang, Y., & Bi, X. (2017). Evaluation of the photooxidation efficiency of As(III) applying the UVC/Oxalate technique. *Chemosphere, 182*, 356–363.

Jiang, H., Zhu, C. Q., Yuan, Y., Yue, C. L., Ling, C., Liu, F. Q., & Li, A. M. (2020). Enhanced activation of peroxymonosulfate with metal-substituted hollow $M_xCo_{3-x}S_4$ polyhedrons for superfast degradation of sulfamethazine. *Chemical Engineering Journal, 384*, 123302.

Lan, Q., Li, F. B., Sun, C. X., Liu, C. S., & Li, X. Z. (2010). Heterogeneous photodegradation of pentachlorophenol and iron cycling with goethite, hematite and oxalate under UVA illumination. *Journal of Hazardous Materials, 174*, 64–70.

Lan, Q., Cao, M., Ye, Z., Zhu, J., Chen, M., Chen, X., & Liu, C. (2016). Effect of oxalate and pH on photodegradation of pentachlorophenol in heterogeneous irradiated maghemite system. *Journal of Photochemistry and Photobiology A: Chemistry, 328*, 198–206.

Li, X., Zhou, M. H., & Pan, Y. W. (2018a). Enhanced degradation of 2,4-dichlorophenoxyacetic acid by premagnetization Fe-C activated persulfate: Influential factors, mechanism and degradation pathway. *Journal of Hazardous Materials, 353*, 454–465.

Li, X., Zhou, M. H., & Pan, Y. W. (2018b). Enhanced degradation of 2,4-dichlorophenoxyacetic acid by premagnetization Fe-C activated persulfate: Influential factors, mechanism and degradation pathway. *Journal of Hazardous Materials, 353*, 454–465.

Li, J., Li, Y. J., Xiong, Z. K., Yao, G., & Lai, B. (2019). The electrochemical advanced oxidation processes coupling of oxidants for organic pollutants degradation: A mini-review, Chinese Chem. *Lett., 30*, 2139–2146.

Li, X., Jia, Y., Zhou, M. H., Su, X. F., & Sun, J. H. (2020a). High-efficiency degradation of organic pollutants with Fe, N co-doped biochar catalysts via persulfate activation. *Journal of Hazardous Materials, 397*, 122764.

Li, J. F., Liu, H. J., Lan, H. C., Ji, Q. H., An, X. Q., Liu, R. P., & Qu, J. H. (2020b). A promising treatment method for Cr(VI) detoxification and recovery by coupling $Fe^0/Fe_3C/C$ fine powders and circulating fluidized bed. *Chemical Engineering Journal, 398*, 125565.

Pan, Y. W., Zhou, M. H., Li, X., Xu, L. T., Tang, Z. X., & Liu, M. M. (2016). Novel Fenton-like process (pre-magnetized Fe^0/H_2O_2) for efficient degradation of organic pollutants. *Separation and Purification Technology, 169*, 83–92.

Pan, Y. W., Zhou, M. H., Cai, J. J., Tian, Y. S., & Zhang, Y. (2019). Mechanism study of nitrilotriacetic acid-modified premagnetized Fe^0/H_2O_2 for removing sulfamethazine. *Chemical Engineering Journal, 374*, 1180–1190.

Pan, Y. W., Wang, Q., Zhou, M. H., & Cai, J. J. (2020a). Tian Y.S., Zhang Y., Kinetic and mechanism study of UV/pre-magnetized-Fe^0/oxalate for removing sulfamethazine. *Journal of Hazardous Materials, 398*, 122931.

Pan, Y. W., Zhou, M. H., Wang, Q., Cai, J. J., Tian, Y. S., & Zhang, Y. (2020b). EDTA, oxalate, and phosphate ions enhanced reactive oxygen species generation and sulfamethazine removal by zero-valent iron. *Journal of Hazardous Materials, 391*, 122210.

Repo, E., Koivula, R., Harjula, R., & Sillanpää, M. (2013). Effect of EDTA and some other interfering species on the adsorption of Co(II) by EDTA-modified chitosan. *Desalination, 321*, 93–102.

Song, K., Mohseni, M., & Taghipour, F. (2019). Mechanisms investigation on bacterial inactivation through combinations of UV wavelengths. *Water Research, 163*, 114875.

Wang, J. L., & Chen, H. (2020). Catalytic ozonation for water and wastewater treatment: Recent advances and perspective. *Science of The Total Environment, 704*, 135249.

Xu, L. J., Qi, L. Y., Sun, Y., Gong, H., Chen, Y. L., Pei, C., & Gan, L. (2020a). Mechanistic studies on peroxymonosulfate activation by g-C_3N_4 under visible light for enhanced oxidation of light-inert dimethyl phthalate. *Chinese Journal of Catalysis, 41*, 322–332.

Xu, L. J., Zhang, X. M., Han, J. G., Gong, H., Meng, L., Mei, X., Sun, Y., QiL, Y., & Gan, L. (2020b). Degradation of emerging contaminants by sono-Fenton process with in situ generated H_2O_2 and the improvement by P25-mediated visible light irradiation. *Journal of Hazardous Materials, 391*, 122229.

Zhang, C., Ren, G. B., Wang, W., Yu, X. M., Yu, F. K., Zhang, Q. Z., & Zhou, M. H. (2019a). A new type of continuous-flow heterogeneous electro-Fenton reactor for tartrazine degradation. *Separation and Purification Technology, 208*, 76–82.

Zhang, H., Ji, Q. Q., Lai, L. D., Yao, G., & Lai, B. (2019b). Degradation of p-nitrophenol (PNP) in aqueous solution by mFe/Cu-air-PS system, Chinese Chem. *Lett., 30*, 1129–1132.

Zhou, T., Wu, X., Mao, J., Zhang, Y., & Lim, T. T. (2014). Rapid degradation of sulfonamides in a novel heterogeneous sonophotochemical magnetite-catalyzed Fenton-like (US/UV/Fe_3O_4/oxalate) system. *Applied Catalysis B: Environmental, 160-161*, 325–334.